Growth and structure of an ultrathin tin oxide film on Rh(111)

J. Yuhara, D. Tajima, T. Matsui, K. Tatsumi, S. Muto, M. Schmid, and P. Varga

Citation: Journal of Applied Physics **109**, 024903 (2011); doi: 10.1063/1.3537871
View online: http://dx.doi.org/10.1063/1.3537871
View Table of Contents: http://scitation.aip.org/content/aip/journal/jap/109/2?ver=pdfcov
Published by the AIP Publishing

Growth and structure of an ultrathin tin oxide film on Rh(111)

J. Yuhara,[1,a)] D. Tajima,[1] T. Matsui,[1] K. Tatsumi,[1] S. Muto,[1] M. Schmid,[2] and P. Varga[2]
[1]*School of Engineering, Nagoya University, Furo-cho, Chikusa-ku, Nagoya, 464-8603, Japan*
[2]*Institut für Allgemeine Physik, Technische Universität Wien, Wiedner Hauptstraße 8-10, A-1040 Wien, Austria*

(Received 21 November 2010; accepted 9 December 2010; published online 20 January 2011)

The oxidation of submonolayer tin films on a Rh(111) surface by O_2 gas was studied using low energy electron diffraction, Auger electron spectroscopy, x-ray photoemission spectroscopy (XPS), and scanning tunneling microscopy. A uniform tin oxide monolayer film formed at oxidation temperatures around 500 °C and a partial pressure of 2×10^{-7} mbar O_2. The tin oxide film had (2×2) periodicity on the Rh(111) surface, and the resulting tin coverage was determined to be 0.5 ML. Using XPS, the compositional ratio O/Sn was determined to be 3/2. XPS spectra showed a single component for the Sn and O peaks, indicating a uniform bonding environment. Finally, *ab initio* density-functional theory total energy calculations and molecular dynamics simulations were performed using the projector augmented wave method to determine the detailed structure of the tin oxide thin film. © *2011 American Institute of Physics*. [doi:10.1063/1.3537871]

I. INTRODUCTION

Metal oxide thin films that grow on crystalline substrates often differ from bulk oxides. The structures of the thin films are affected by the atomic arrangement and chemical reactivity of the substrate surfaces, and the resulting metal oxide films have unique interatomic distances, structural symmetry, and surface reactivity compared to the metal oxide substrate. The oxidation of tin films on metallic surfaces, such as Au(111),[1–4] Pt(111),[5] $Pt_3Sn(111)$,[6–8] and Pd(111),[9] has been recently studied both fundamentally and also for its industrial applications, e.g., as applied to gas sensors, catalysis, and transparent electrodes. All these substrates are less reactive against O_2 gas than the tin films, resulting in the formation of commensurate overlayer tin oxide films. The oxidation of a tin film on Pt(111) and $Pt_3Sn(111)$ surfaces yields an ultrathin tin oxide film that exhibits a (4×4) pattern with low energy electron diffraction (LEED).[5,6,8] On the contrary, a $c(2\times4)$ pattern is formed in the case of a Au(111) surface.[3]

In order to distinguish the effects of the substrate chemical reactivity from the atomic distance of the substrate atoms on the formation of an ultrathin tin oxide film structure, it is necessary to examine different substrates with the same structural symmetry and interatomic distances. Rh(111) is an ideal substrate for comparing the chemical reactivity with Pt(111), since they share an identical structural symmetry; both are face centered cubic (111) surfaces, and their interatomic distances are very similar (the Rh lattice is about 3% smaller).

We performed a combined experimental and theoretical study on the growth and structure of ultrathin tin oxide films on Rh(111). The growth processes and the evaluation of the surface structures were examined using LEED, scanning tunneling microscopy (STM), Auger electron spectroscopy (AES), and x-ray photoemission spectroscopy (XPS). The combined analysis identified the structure as a (2×2) pattern, and determined that the tin coverage was 0.5 ML and the compositional ratio O/Sn was 3/2. Using these results, the structure of the film was investigated theoretically by *ab initio* density-functional theory (DFT) total energy calculations and molecular dynamics (MD) simulations.

II. EXPERIMENT AND CALCULATION

The work was performed using two very similar ultrahigh-vacuum systems, one in Nagoya and the other in Vienna. Each system consisted of a preparation chamber with a base pressure below 2×10^{-10} mbar, and an analysis chamber with a base pressure below 10^{-10} mbar. They were equipped with four-grid LEED optics, an electron gun, an x-ray source, a hemispherical analyzer used in AES and XPS, and STM. First, the Rh(111) crystal surfaces were cleaned in the preparation chamber by 2 keV Ar^+ ion sputtering; this was followed by annealing to 800 °C. The cleanliness and quality of the Rh surfaces were checked by AES and LEED in the analysis chamber. No contamination such as from C and O was observed within the detection limits.

The clean Rh(111) surface exhibited a distinct (1×1) LEED pattern. Submonolayer tin films (0.2 to 1.0 monolayer) were deposited on the Rh(111) surface at room temperature [we define one monolayer (ML) to be an overlayer having the atomic density of a Rh(111) layer). The deposition rate was monitored using a quartz crystal microbalance. After deposition, the tin films on the Rh(111) surface were annealed at temperatures between 300 and 600 °C in O_2 at a partial pressure between 2×10^{-6} and 2×10^{-8} mbar, and were cooled to room temperature at the same oxygen pressure. The surface structure and elemental concentrations of these tin oxide films were investigated by LEED, AES, and XPS. The AES peak-to-peak heights were converted into concentrations using the sensitivity factors 0.80 for Sn (432 eV), 0.50 for O (503 eV), and 0.65 for Rh (305 eV).[10] XPS data were recorded with a VG CLAM2 analyzer using a Mg K_a x-ray source ($h\nu$=1253.6 eV). The overall resolution

a)Electronic mail: j-yuhara@nagoya-u.jp.

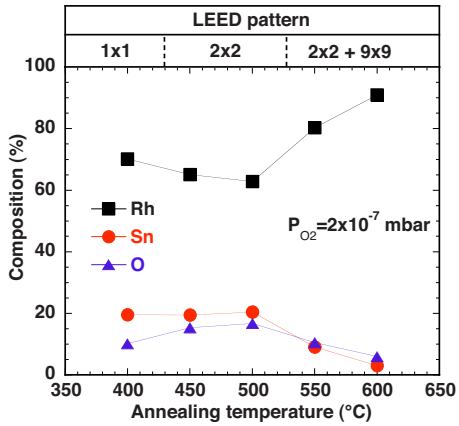

FIG. 1. (Color online) Oxidation temperature dependence of the surface composition and LEED patterns of the (Sn,O)/Rh(111) system.

of the spectrometer was 0.1 eV. A SnO_2 bulk specimen was used as a standard sample for the XPS measurements, which was used to estimate the compositional ratio O/Sn of the tin oxide film on Rh(111). STM measurements were performed using a customized Omicron room temperature micro-STM in Vienna, and a customized UNISOKU room temperature STM in Nagoya. These were the same instruments used in Refs. 11 and 12, respectively. All STM images were obtained in constant current (I_t=0.5 nA) mode with the sample negative (V_s=−1.0 to −0.01 V).

Ab initio DFT total energy calculations were performed to study the detailed structural determination of the tin oxide film, using the Vienna *ab initio* simulation package (VASP).[13] These calculations used the projector augmented wave method to describe the interaction between the electrons and ions.[14] The calculations had a plane wave cutoff of 250 eV and generalized gradient corrections.[15] The forces acting on particular atoms were smaller than 0.05 eV/Å in the structural optimization. To examine the total energy, a grid was chosen that corresponds to 10×10×1 k points in the primitive surface cell. With this setup, we estimated that the typical errors in the calculation of the adsorption energy were less than 10 meV per adatom. The structural model was initially obtained using simulated annealing in the MD simulation. The temperature was decreased from 1500 to 500 K. There were 5000 steps with a time step of 1.0 fs/step. Details about the MD program are provided elsewhere. The *ab initio* DFT total energy calculations were subsequently performed to determine the tin oxide structure.

III. RESULTS

Figure 1 show the dependence of the surface composition as measured by AES and LEED patterns for the 0.5 ML tin film on Rh(111). The film has been oxidized at different temperatures. The LEED patterns exhibited a distinct c(2×4) pattern before annealing, which is consistent with a previous study.[11] The tin film was annealed in an oxygen atmosphere of 2×10^{-7} mbar for 10 min at temperatures from 400 to 600 °C. The tin peak maintained a constant intensity in the AES spectra up to 500 °C while the oxygen peak increased up to 500 °C. As shown in Fig. 1, when the temperature is under 400 °C, a (1×1) LEED pattern was

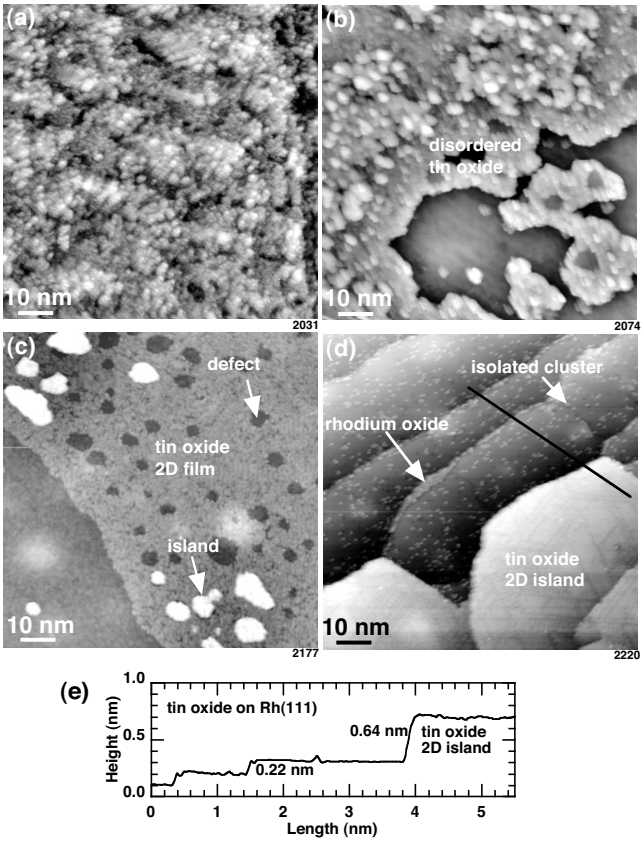

FIG. 2. Large-scale STM images of tin oxide films on a Rh(111) surface after annealing at temperatures of (a) 300, (b) 400, (c) 500, and (d) 600 °C. (e) is a section profile along the black line in (d).

observed while for higher temperatures (450–500 °C), a clear (2×2) LEED pattern was observed. Thus, the tin film appears to be fully oxidized around 500 °C. While the tin coverage was deposited between 0.25 to 1 ML, the (2×2) LEED spots at 0.5 ML become the sharpest. Both the Sn and O concentrations started to decrease at an oxidation temperature above 550 °C. After annealing in the oxygen atmosphere at higher temperatures, a faint (9×9) pattern characteristic of the trilayer oxide on Rh(111) (Ref. 17) was found, in addition to the (2×2) spots. This meant that the Rh(111) surface that was not covered by the tin film started to oxidize.

Figures 2(a)–2(d) show STM images of tin oxide films on a Rh(111) surface formed by the Sn deposition of 0.5 ML and annealing in oxygen at temperatures of 300 °C, 400 °C, 500 °C, and 600 °C, respectively. We see disordered films after oxidization at 300 °C. Tin oxide monolayer films start to grow at 400 °C [Fig. 2(b)] while still coexisting with the disordered areas. An area not covered by the tin oxide films is also seen in the figure. At a temperature of 500 °C, an almost uniform tin oxide overlayer formed, although defects and islands are also seen on the terrace. After oxidation at 600 °C, the tin oxide two-dimensional (2D) films started to shrink, and many isolated clusters of unknown identity were found on the rhodium terraces. We also see dark lines on the tin oxide 2D islands and the rhodium trilayer oxide[17] at the step edges. The section profile at the line in the STM image from Fig. 2(d) is shown in Fig. 2(e). The step height forming

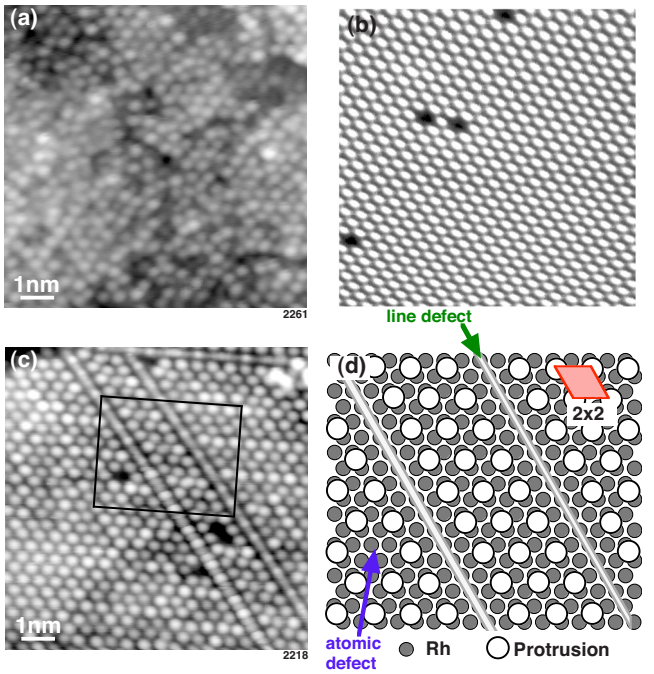

FIG. 3. (Color online) Atomically resolved STM images of tin oxide films on a Rh(111) surface after annealing at temperatures of (a) 400, (b) 500, and (c) 600 °C. (d) A schematic illustrating of the protrusions extracted from (c).

a tin oxide film only on an upper terrace was obtained to be 0.62 nm. Since the step height is sum of the thickness of the tin oxide film and monatomic step height of Rh(111), which are 0.22 nm, the thickness of the tin oxide film was determined to be 0.40 nm. When the initial amount of tin deposition was less than 0.5 ML, the tin oxide film partially covered the surface. Thus, the nominal Sn coverage for the tin oxide film was estimated to be 1/2 ML.

In order to identify the role of rhodium atoms in the tin oxide film, a Sn–Rh surface alloy with a $(\sqrt{3}\times\sqrt{3})$ superstructure was prepared by a deposition of 0.5 ML Sn on Rh(111), followed by annealing at 500 °C for 5 min. Then, the Sn–Rh surface alloy was annealed at 500 °C in an oxygen atmosphere of 2×10^{-7} mbar. The LEED pattern showed faint (9×9) spots, and no spots of (2×2) were observed. Therefore, once Sn and Rh form the surface alloy at the Rh(111) surface, Sn will not contribute an overlayer tin oxide film.

Figures 3(a)–3(c) show atomic resolution STM images of the tin oxide 2D film or island on a Rh(111) surface after annealing at 400 °C, 500 °C, and 600 °C, respectively. Bright spots are visible in a locally hexagonal arrangement at 400 °C, which indicates that tin oxide films start ordering at the atomic scale. At 500 °C, an atomically flat and uniform tin oxide film was formed, with atomic defects observed locally. From the atomic distance of these bright spots, it was determined that they were arranged in a (2×2) pattern. When the annealing temperature was above 500 °C, the tin oxide film started to shrink [Fig. 2(d)] and line defects became observable in addition to the atomic defects in tin oxide 2D islands. Figure 3(d) shows a schematic illustration of the protrusions, atomic defects, and line defects extracted from Fig. 3(c).

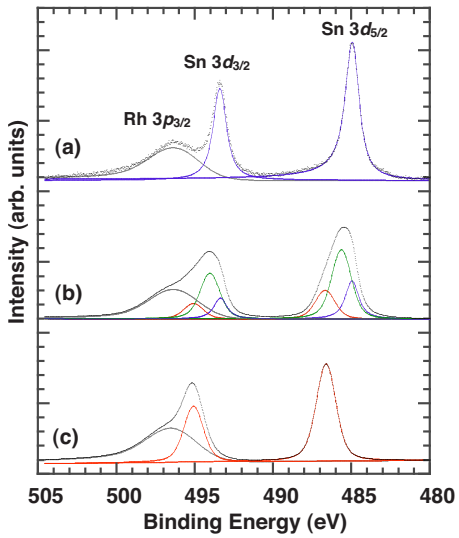

FIG. 4. (Color online) XPS spectra at the Sn $3d$ and Rh $3p$ core levels of 0.4 ML of Sn film on Rh(111) at RT (a), and after annealing in an O_2 gas atmosphere at 400 (b) and 500 °C (c). Fitted metal, oxide, and intermediate Gaussian components are also shown.

Figure 4 shows Sn $3d$ XPS spectra before and after annealing a tin film, at both 400 and 500 °C in an O_2 gas atmosphere. The binding energy of Sn $3d_{5/2}$ for a tin film on Rh(111) was shown to be at 485.0 eV. It is clear that the Sn $3d_{3/2}$ spectrum overlapped with the Rh $3p_{3/2}$ spectrum. The Sn $3d_{5/2}$ spectrum exhibited three components after annealing at 400 °C. When the specimen was annealed at 500 °C, the Sn spectrum showed a single component at a peak energy of 486.7 eV. It is considered that tin films are fully oxidized at a temperature of 500 °C. The two components with peak energies of 485.0 eV and 486.7 eV were determined to be a metallic tin film and tin oxide film, respectively. The component with energy at 485.6 eV is considered to be the intermediate oxide state.

The O $1s$ XPS spectra were also obtained, as shown in Fig. 5. After annealing at 400 °C, the O $1s$ spectrum exhibited two components at the peak energies of 530.4 eV and 531.1 eV, which were an intermediate partial oxide state and a fully oxide state, respectively. When the annealing temperature increased to 500 °C, the O $1s$ spectrum showed

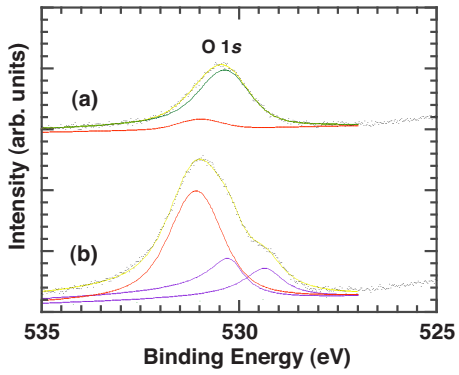

FIG. 5. (Color online) XPS spectra at the O $1s$ core level after annealing the 0.4 ML of Sn film on Rh(111) in an O_2 gas atmosphere at 400 (a) and 500 °C (b). Fitted tin oxide, rhodium oxide, and intermediate Gaussian components are also shown.

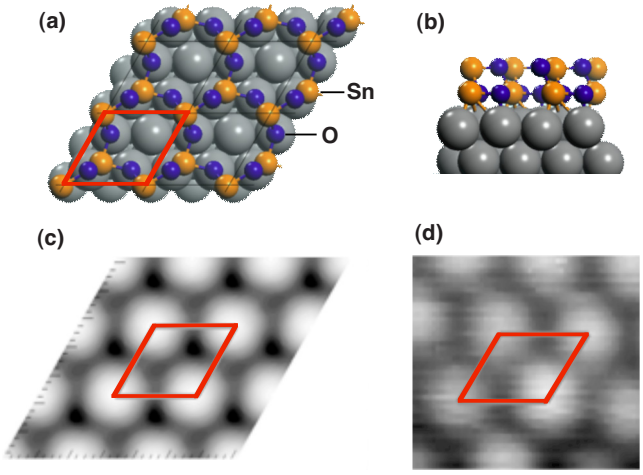

FIG. 6. (Color online) (a) Top and (b) side views of the most stable Sn_2O_3 structure on Rh(111) obtained by DFT. (c) Simulated STM image of the Sn_2O_3 film as obtained by the Tersoff–Hamann approach in (a). (d) STM image of the Sn_2O_3 film on Rh(111).

three components at the peak energies of 531.1, 530.2, and 532.9 eV. The main component of 531.1 eV originated from the tin oxide film, and the remaining components were from the trilayer oxide on Rh(111).[17] Therefore, the surface was not completely covered by the tin oxide film, and some part of the rhodium surface was oxidized. The compositional ratio O/Sn for the tin oxide film was estimated to be 1.45, using the area intensity of the Sn $3d_{5/2}$ and O $1s$ components of the tin oxide film in comparison with the XPS spectrum of the SnO_2 bulk specimen.

We now examine the structure of the tin oxide film in more detail. As already confirmed by LEED and STM, the tin oxide film forms a (2×2) structure. The tin coverage was determined to be 0.5 ML using AES. The compositional ratio O/Sn was determined to be 3/2 by XPS. Using these experimental facts, we surveyed the structural model by the simulated annealing of MD simulation. The structural model that showed minima in the simulated annealing was examined by *ab initio* total energy calculations to obtain the energetically most stable tin oxide structure. Figure 6 shows the energetically most stable tin oxide structure on Rh(111). It is seen that the tin oxide film forms a bilayer honeycomb structure. The simulated STM image, as obtained by the Tersoff–Hamann approach,[16] showed good consistency with the experimental STM image, as seen in Figs. 6(c) and 6(d), respectively. It is also found that the bright spot correspond to the position of Sn atoms at the upper layer.

IV. DISCUSSION

Oxidation of the tin film on a Rh(111) surface shows a periodic (2×2) superstructure. The (2×2) superstructure appears to be due to an ultrathin tin oxide film on Rh(111), since the superstructures differ for rhodium oxide on a Rh(111) surface ((9×9) superstructure[17]) and the surface alloy formation of tin on a Rh(111) surface ($(\sqrt{3}\times\sqrt{3})R30°$ superstructure[18]). While the (2×2) structure indicates that the Sn coverage is 1/4, 1/2, or 3/4 ML, the (2×2) LEED spots become the sharpest at a coverage of 0.5 ML. The STM image also indicates that the nominal tin coverage is 0.5 ML.

Since the oxidation of the Sn–Rh surface alloy on the Rh(111) substrate shows a (9×9) LEED pattern, it appears that tin atoms cannot be formed in the oxygen atmosphere, if tin atoms are incorporated within the Rh(111) substrate. These results indicate that the tin oxide film is an overlayer film. Since the bond enthalpies are 532 kJ/mol for Sn–O and 405 kJ/mol for Rh–O, and considering that the Rh–Rh bond is much stronger than the Sn–Sn bond, Rh is much less likely to oxidize than Sn. This also suggests that a "true" tin oxide is much more likely to occur than a Sn–Rh oxide. However, if stronger oxidants like ozone or nitrous oxide are exposed to a Sn–Rh surface alloy, a ternary surface oxide might be formed, like the Sn–Pt surface alloy.[5,19]

The STM images indicate that 2D tin oxide islands start to grow, not from the step edge but randomly from the terraces. However, these tin oxide 2D islands shrink from the outside at oxidizing temperatures above 550 °C. Although the LEED patterns show the (2×2) spots above 500 °C, the STM images at atomic resolution show that a (2×2) superstructure is locally formed even at 400 °C [Fig. 3(a)]. The LEED pattern shows that almost perfect ordering is reached at 500 °C.

Close inspection of the image shows that the protrusions do not form a perfect (2×2) ordered lattice at a position close to the line defects; however, some atoms are slightly shifted from their position in an equidistant lattice. We also find that the distance between the protrusions in the (2×2)-like areas next to the line defects is often shorter than the distance in a perfect (2×2) pattern. This possibly indicates a preference of the film to form a structure with a lattice constant that is slightly shorter than that of an ideal (2×2) structure, or provides for some defects, e.g., oxygen vacancies. From the structural model shown in Fig. 6, it is considered that the line and atomic defects arise from the missing of the upper Sn atoms, whose positions correspond to the bright spots. The STM image along the line defects indicates a local rearrangement of lower Sn atoms and the surrounding O atoms.

The STM images show one protrusion (bright spot) per (2×2) unit cell. In the case of tin oxide films on Pt(111) and $Pt_3Sn(111)$ surfaces, protrusions in the STM images are located at Sn positions.[5,6,8] In comparison with the STM image and the simulated image of the optimized Sn_2O_3 film structure, the protrusions in the STM images here are also found to the Sn positions as well. Only one of the two Sn atoms is visible in the STM, since these Sn atoms form a bilayer film.

The binding energy of the Sn $3d_{5/2}$ peak for the tin film on Rh(111) is determined to be 485.0 eV, which corresponds well to a metallic Sn^0 state.[20] When the tin film is oxidized on Rh(111), the Sn $3d_{5/2}$ peak shifts to the higher binding energy of 486.7 eV. The single component for the peak indicates a uniform bonding environment. This is consistent with the bilayer honeycomb structural model that every Sn atom is bound to three O atoms. Because the Sn $3d_{5/2}$ peaks for the SnO_2 and SnO substrates occur at 487.1 eV and 486.2 eV, respectively,[21] the tin oxide film shows Sn $3d_{5/2}$ peaks be-

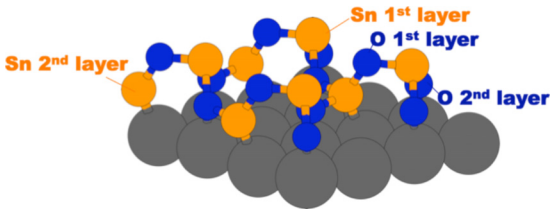

FIG. 7. (Color online) Bird's eye view of the Sn_2O_3 film on Rh(111).

tween these values. Therefore, we conclude that the composition of the tin oxide film is Sn_2O_3. This result is in good agreement with the peak areal intensity analysis for the tin oxide film and the standard SnO_2 bulk specimen. In the present study, the intermediate state with a peak at 485.6 eV is considered to be the SnO film. From these results, the binding energies of the 1*s* peak for the Sn_2O_3 and SnO films are also determined to be 531.1 eV and 530.4 eV, respectively. These O peaks showed a single component, which indicates a uniform bonding environment.

The energetically most stable tin oxide structure has been obtained by *ab initio* total energy calculations using experimental results: a (2×2) structure with two tin atoms in the unit cell, and a compositional ratio O/Sn of 3/2. Figure 6 shows that the Sn_2O_3 obtains a bilayer honeycomb structure. The thickness of the Sn_2O_3 film is estimated from DFT calculations to be 0.38 nm, which is in good agreement with the height of 0.40 nm obtained from the STM image. Each O atom is bound to two Sn atoms; one at the upper layer and the other at the lower layer. The bonding direction of each O atom is either parallel or perpendicular to the surface. Thus, the O atoms stabilize the bilayer structure (Fig. 7).

The SnO and rutile SnO_2 structures with their (111) faces have nearly triangular unit cells, with side lengths of 538 and 615 pm for SnO, and 571 and 670 p.m. for SnO_2. The angles of the unit vectors at the (111) faces for SnO and SnO_2 are 64° and 72°, respectively. Since the tin oxide films are formed on a Rh(111) surface with an atomic distance of 269 pm, the films form a (2×2) structure that has a smaller triangular unit cell, with dimensions 538 pm$\times$538 pm Also, in contrast to the (111) planes of bulk oxides, the tin oxide film forms an equilateral triangle structure consistent with the Rh(111) surface.

The surface structure of tin oxide films on Rh(111) is found to differ from those formed on $Pt_3Sn(111)$, Pt(111), and Au(111) surfaces.[1–8] Especially, it is interesting to observe various tin oxide superstructures on Rh(111) and Pt(111) surfaces, since the lattice constants of these metals are very similar: 0.27 nm and 0.28 nm, respectively (the Rh lattice is about 3% smaller). The different superstructures formed on different substrates seem to be closely related to the chemical reactivity of the substrate. It has been found that Sn atoms form overlayer films of a $c(2\times4)$ structure on a Rh(111) surface at room temperature,[11] while Sn atoms react and mix with Pt atoms on a Pt(111) surface.[7] This possibly indicates that the chemical reactivity of Pt–Sn is higher than that of Rh–Sn, which may result in more complex surface reconstructions for tin oxide films on a Pt(111) surface.[5,6,8]

V. SUMMARY

Commensurate monolayer tin oxide films with $p(2\times2)$ symmetry were formed on a Rh(111) surface, in an oxygen atmosphere of 10^{-7} mbar at temperatures around 450–500 °C. The tin coverage for the uniform tin oxide film was estimated to be 0.5 ML, using a combined analysis of LEED-AES-STM. Using XPS, the compositional ratio Sn/O was estimated to be 2/3. Using these experimental results, the simulated annealing and *ab initio* DFT total energy calculations were performed to obtain the energetically most stable structure. It was found that the Sn_2O_3 film forms a bilayer structure. An O atom bridge is bound to two Sn atoms; one in the upper layer and the other in the lower layer. Although the lattice constants for Rh(111) and Pt(111) are very similar, the surface structures of the tin oxide films were found to be totally different from each other. This is due to the chemical reactivity of the Rh and Pt atoms with the Sn atoms.

ACKNOWLEDGMENTS

One of the authors (J.Y.) gratefully acknowledges financial support by the bilateral program for scientist exchange between Federal Ministry of Science and Transport of Austria (FMST) and the Japan Society for Promotion of Science (JSPS). This work was partially supported by Austrian Fonds zur Förderung der wissenschaftlichen Forschung. This work was partially supported by Grant-in-Aid for Scientific Research on Priority Areas (Grant No. 22013008) of Ministry of Education, Culture, Sports, Science and Technology (MEXT), Japan. We are grateful to Dr. T. Yamazaki for providing a SnO_2 bulk specimen.

[1] Y. Zhang and A. J. Slavin, J. Vac. Sci. Technol. A **10**, 2371 (1992).
[2] Y. Zhang and A. J. Slavin, Phys. Rev. B **49**, 2005 (1994).
[3] Y. Zhang and A. J. Slavin, Surf. Sci. **328**, 181 (1995).
[4] J. W. Yan, Z. X. Xie, Z. X. Cao, C. J. Zhou, J. Y. Kang, and B. W. Mao, Chem. Phys. Lett. **373**, 575 (2003).
[5] M. Batzill, D. E. Beck, and B. E. Koel, Phys. Rev. B **64**, 245402 (2001).
[6] M. Batzill, J. Kim, D. E. Beck, and B. E. Koel, Phys. Rev. B **69**, 165403 (2004).
[7] D. I. Jerdev and B. E. Koel, Surf. Sci. **492**, 106 (2001).
[8] M. Hoheisel, S. Speller, W. Heiland, A. Atrei, U. Bardi, and G. Rovida, Phys. Rev. B **66**, 165416 (2002).
[9] A. F. Lee and R. M. Lambert, Phys. Rev. B **58**, 4156 (1998).
[10] L. E. Davis, N. C. MacDonald, P. W. Palmberg, G. E. Riach, and R. E. Weber, *Handbook of Auger Electron Spectroscopy*, 2nd ed. (Physical Electronics Industries, Eden Prairie, Minnesota, 1976).
[11] J. Yuhara, M. Schmid, and P. Varga, Phys. Rev. B **67**, 195407 (2003).
[12] J. Yuhara, T. Takada, D. Nakamura, K. Soda, and M. Kamada, Mater. Sci. Eng., B **96**, 145 (2002).
[13] G. Kresse and J. Furthmuller, Phys. Rev. B **54**, 11169 (1996).
[14] G. Kresse and D. Joubert, Phys. Rev. B **59**, 1758 (1999).
[15] J. P. Perdew, J. A. Chevary, S. H. Vosko, K. A. Jackson, M. R. Pederson, D. J. Singh, and C. Fiolhais, Phys. Rev. B **46**, 6671 (1992).
[16] J. Tersoff and D. R. Hamann, Phys. Rev. B **31**, 805 (1985).
[17] J. Gustafson, A. Mikkelsen, M. Borg, E. Lundgren, L. Köhler, G. Kresse, M. Schmid, P. Varga, J. Yuhara, X. Torrelles, C. Quirós, and J. N. Andersen, Phys. Rev. Lett. **92**, 126102 (2004).
[18] Y. Li, M. R. Voss, N. Swami, Y.-L. Tsai, and B. E. Koel, Phys. Rev. B **56**, 15982 (1997).
[19] N. A. Saliba, Y. L. Tsai, and B. E. Koel, J. Phys. Chem. B **103**, 1532 (1999).
[20] P. Hanys, P. Janecek, V. Matolin, G. Korotcenkov, and V. Nehasil, Surf. Sci. **600**, 4233 (2006).
[21] J. M. Themlin, M. Chtaib, L. Henrard, P. Lambin, J. Darville, and J. M. Gilles, Phys. Rev. B **46**, 2460 (1992).